

Summarize the Past to Predict the Future: Natural Language Descriptions of Context Boost Multimodal Object Interaction Anticipation

Razvan-George Pasca¹ Alexey Gavryushin¹ Yen-Ling Kuo² Otmar Hilliges¹ Xi Wang¹
¹ETH Zürich ²Massachusetts Institute of Technology

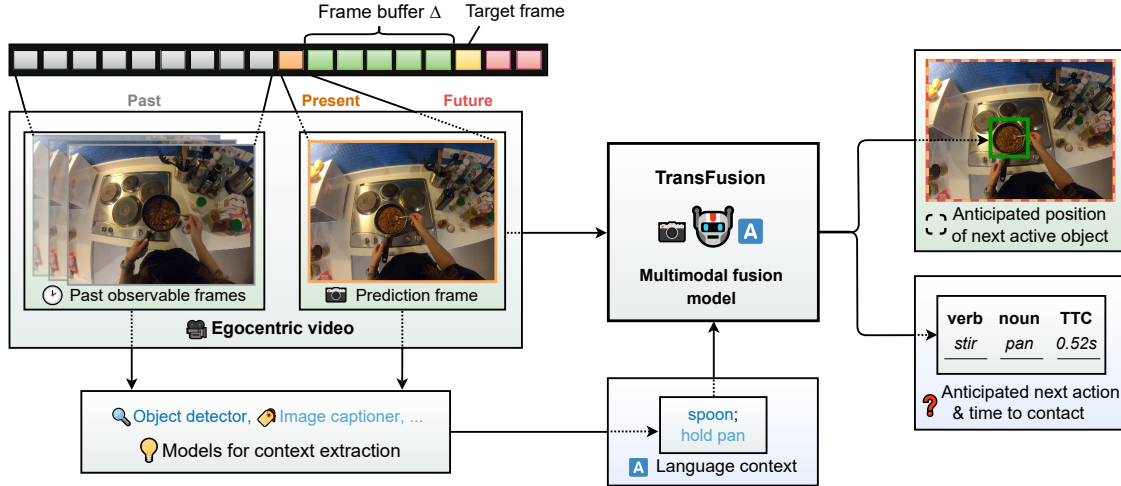


Figure 1. **Multimodal fusion transformer for short-term object interaction prediction.** Given a video sequence from the past observation, the object interaction prediction task aims to predict a set of objects that will be interacted with in the future that is Δ frames apart from the current prediction frame. The output includes the bounding box, the associated action described by a verb-noun pair, and the time to contact for each predicted object. We propose TransFusion that uses language summary of past action context, a more compact representation than video features, to help the prediction of future object interaction. Our approach allows the model to efficiently aggregate past observations, to explicitly represent action context, and to better reason about future interactions, especially on a semantic level.

Abstract

We study the task of object interaction anticipation in egocentric videos. Successful prediction of future actions and objects requires an understanding of the spatio-temporal context formed by past actions and object relationships. We propose TransFusion, a multimodal transformer-based architecture, that effectively makes use of the representational power of language by summarizing past actions concisely. TransFusion leverages pre-trained image captioning models and summarizes the caption, focusing on past actions and objects. This action context together with a single input frame is processed by a multimodal fusion module to forecast the next object interactions. Our model enables more efficient end-to-end learning by replacing dense video features with language representations, allowing us to benefit from knowledge encoded in large pre-trained models. Experiments on Ego4D and EPIC-KITCHENS-100 show the effectiveness of our multimodal

fusion model and the benefits of using language-based context summaries. Our method outperforms state-of-the-art approaches by 40.4% in overall mAP on the Ego4D test set. We show the generality of TransFusion via experiments on EPIC-KITCHENS-100. Video and code are available at: <https://eth-ait.github.io/transfusion-proj/>.

1. Introduction

The ability to predict plausible future human object interactions is an important component of many assistive technologies. Specifically, the task of *short-term object interaction anticipation* [16, 20] is defined as predicting *which* object a user will interact with next and *what* action will be performed, given an egocentric video input. Providing an effective solution to this task would signify an important step towards artificial agents that can assist humans in their daily activities such as virtual assistants or care robots.

This task is challenging because it requires reasoning

about user intent and goals [7, 33, 40], governed by not directly observable cognitive processes. Given the complex and ambiguous nature of human activities, inferring *which* objects will be interacted with and *what* action will be performed, strongly depends on suitable representations of the action’s spatio-temporal context. For example, given a video in which the user holds a vegetable, the most likely next action would be to slice it but only if a knife and cutting board are present. But without these utensils, there is significantly more uncertainty. Therefore, understanding what has happened in the past and how objects relate to each other is critical for object interaction anticipation. We collectively refer to these concepts as *action context*. Existing interaction forecasting methods do not explicitly model action context and rely on neural networks to extract that information from fixed-sized chunks of frames [6, 16, 20, 31]. In this paper, we propose to use language summarization of the past as an explicit representation of action context, which allows the method to focus on objects and actions that are directly relevant to the ongoing and most likely future activities and filters-out ambiguities due to visually cluttered scenes. To this end, we introduce a multimodal fusion approach in which object interaction anticipation is guided by past action context summarized in the form of concise natural language descriptions.

Specifically, we introduce a transformer-based multimodal fusion model, TransFusion. As shown in Figure 1, TransFusion takes language summaries of action context and the current frame of a video as input and predicts future object interactions. We employ existing image captioning systems from which we generate a concise description of past actions described by pairs of verbs and nouns. We use CLIP [35], a multimodal model trained on pairs of images and captions, to detect visible objects in the past frames, and deem them as task-relevant. The verb-noun pairs together with the list of visible objects form the summary of past action context. Leveraging pre-trained language models eliminates the requirement for dataset-specific action annotations and thus increases the generality of the approach. Our method processes the language context summaries in a multimodal fusion module that operates on RGB images and language-based action context descriptions.

We show experimentally that our context summaries can represent different temporal horizons in a more flexible and concise manner than vision-based features on two challenging egocentric datasets, Ego4D [20] and EPIC-KITCHENS-100 (EK100) [9]. Our results indicate significant accuracy improvements on the interaction anticipation task compared to previous state-of-the-art models. On Ego4D [20], our model improves over models pre-trained on large video datasets by 25.6% on the Ego4D challenge validation set and 40.4% on the test set. TransFusion also achieves similar performance compared to video-only base-

lines on EK100 [9].

In summary, our contributions are:

- The concept of leveraging concise language-based summaries of action context.
- TransFusion, a multimodal fusion model for object interaction anticipation that combines action context descriptions and images.
- Experiments on Ego4d show improvements over state-of-the-art methods on the object interaction anticipation task.
- We empirically show that language descriptions can model action context more effectively than video frames.
- We show the generality of TransFusion via experiments on EK100 which does not provide GT object interaction annotations.

2. Related work

Object interaction anticipation. Several work has been proposed to predict future human-object interaction. Furnari et al. [16] first introduced *next-active-object* (NAO) prediction, which predicts the active/not active label for each object using their motion trajectories features but it doesn’t consider action anticipation. Closely related to NAO, Bertasius et al. [6] introduced *action-objects*, which considers objects that capture the human actor’s visual attention or tactile interaction. Bertasius et al. leverage the data from a stereo camera system and a two-stream network to integrate RGB and depth information showing that certain aspects of human actions can be predicted by exploiting the spatial configuration of the objects and the actor’s head position. Their approach is not easily scalable, because they use stereo information about the scene as input,

In addition to different tasks, Liu et al. [31] propose a model that improves NAO prediction by incorporating future hand trajectory modeling. They obtain impressive results using 3D CNNs, confirming that hand motion cues and scene dynamics have important explanatory power in predicting the short-term future. Nonetheless, their approach encounters scaling limitations because additional ground-truth labels for hand trajectories are needed.

More recently, the Ego4D dataset [20] proposed *object interaction anticipation*. Apart from locating the NAO, the task in Ego4D also requires the prediction of associated nouns and verbs, as well as the time to contact (TTC) for the future interacted objects. The Ego4D method uses the current frame and past video frames as input and employs a two-stage approach to learn noun and box prediction first and then the verbs and TTC prediction. Compared to their work, we perform the task in a single pass, by tuning the multimodal fusion module on top of the extracted RGB and language features to learn nouns and verbs jointly, resulting in better performance.

Action anticipation. Besides localizing future object interactions, predicting the next action steps is an equally important task that AI systems need to perform to interact with humans. A longer prediction timespan requires a better grasp of the structure behind the succession of actions. Anticipative Video Transformer (AVT) [18] is one of the best-performing architectures on the EK100 [10] action anticipation benchmark. AVT uses a pre-trained Visual Transformer [14] as the image feature backbone and attends to the previously observed video frames to anticipate future actions. MeMViT [47] improves AVT by exploiting a longer temporal context, highlighting the importance of modeling a long sequence of previous actions. Other model architectures such as recurrent neural networks [17, 48] and multimodal temporal CNNs [26] are also used to model the temporal contexts. Note that these methods are designed for action classification using video data and adapting them for object detection is not trivial.

Vision and language models. Our approach combines visual and language modalities to improve object anticipation. Most recent multimodal architectures are based on Transformer fusion schemes applied on features extracted by various encoders [5, 12, 27]. We follow the spirit by employing self-attention-based modality fusion. Our work differs in one significant aspect: the language features represent the past action context. This serves as an additional signal to disambiguate the actor’s intent given similar visual scenes.

More broadly, there are numerous transformer-based works aimed at learning cross-modal representations between vision and language [24, 29, 35, 42, 43, 51] using terabyte-scale datasets crawled from multiple internet sources. When combined with large language models such as GPT-2 [36], BERT [13], Sentence-BERT [38], and the T5 variants [8, 37], these vision-language models can be applied to several downstream tasks such as VQA [3] and image captioning [49, 50]. Similar to other vision-language models that are trained with large language input, our approach leverages the state-of-the-art image captioning models [46] to provide a consistent description of past actions.

3. Language-guided Prediction

Our goal is to use language descriptions to represent action context in the past and provide guidance and constraint for the short-term object interaction anticipation task. The text summary offers an explicit yet compact representation, which allows us to focus on task-relevant content and filter out important information from the likely cluttered environment. To this end, we propose TransFusion, a transformer-based model that leverages a joint-attention fusion mechanism, to effectively learn from past actions to predict object interactions in the future. In the following, we begin by defining the object interaction anticipation task (Sec. 3.1). Then we show how to generate a summary of past actions

from an egocentric video (Sec. 3.2). Finally, we present our multimodal fusion model TransFusion (Sec. 3.3).

3.1. Task definition

Given a video $\mathcal{V} = \{f_1, \dots, f_T\}$ of length T as input, our goal is to predict the next object interaction \mathcal{O} , in the most recent frame f_T . We call f_T the prediction frame.

As illustrated in Figure 1, the task is to anticipate object interaction in f_T . $\mathcal{O}_T = \{o_1^T, \dots, o_N^T\}$ denotes the set of future object interactions, with $N > 1$ in scenarios where multiple objects are interacted with simultaneously. In other words, multiple o_i^T can be detected in the same frame f_T . For example, $N = 2$ when one hand is holding two mugs in the kitchen or the left hand is touching a plant while the right hand is moving a pot in the garden. Each object interaction $o_i^T = (b_i^T, n_i^T, v_i^T, t_i^T)$ consists of the object bounding box b_i^T , the semantic object label (noun) n_i^T , the action label (verb) v_i^T , and the time to contact t_i^T . The task is to predict the next active object location b_i^T in the prediction frame f_T , the associated action described by the verb-noun pair (n_i^T, v_i^T) , and the time t_i^T to the point of contact when the interaction is going to start. The task is set up such that the actual object interaction takes place after a buffer time Δ on frame $f_{T+\Delta}$ and the predicted time to contact $t_i^T = \Delta$. Ego4d uses $\Delta \geq 0.33s$. Such a setup requires an element of anticipating future actions and increases the task difficulty.

3.2. Pre-processing: Summarizing the past

Anticipating object interactions requires an understanding of what has happened in the past, which is what we call *action context*. We infer this directly from egocentric video recordings. Inspired by the label format used in egocentric video datasets [9, 20], we aim to describe action context by the associated verb and noun pairs (e.g. “wash tomato”, “cut carrot”). Using the video frames as input, our model first extracts the action context for each frame and then aggregates them over the entire sequence, resulting in segments that correspond to atomic actions.

Extracting action context for individual frames. For each observable video frame f_t , we extract the corresponding action context represented by one verb-noun pair (n^t, v^t) . We first use an off-the-shelf image captioning model [46] to generate multiple captions for each frame of interest, as a means of reducing noise. We then perform part-of-speech tagging [2] and collect all verbs followed by nouns within some maximum distance d , in our case $d = 4$. The most frequently occurring pair is then selected. In the case of ties, the pair with words closer to each other in the sentence is selected, and additionally, the first pair that appears in the sentence is chosen.

As active objects are most commonly in contact with hands, the sequence of objects held by hands may be indicative of the overall task and can help us to better infer

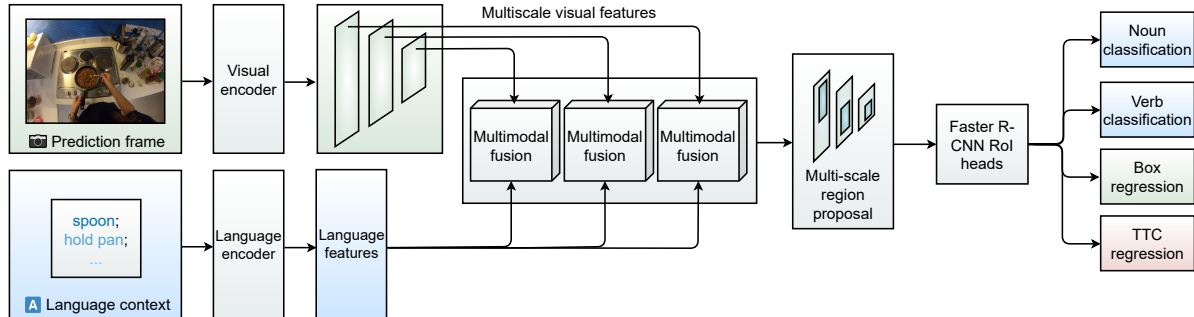


Figure 2. **Overview of the proposed TransFusion model.** TransFusion takes the prediction frame and the summary of past actions as input and predicts the bounding box of the next-active object, the noun-verb pair describing the associated action, and the time to contact. As an example shown here, we use a context length of one. Feature maps of different scales are extracted from the visual encoder and then fused via a multimodal fusion module with the encoded language features. Their output is then processed by a regular feature pyramid network (FPN), denoted as multi-scale region proposal networks, before being fed into the Faster R-CNN detector.

the immediate next steps. Motivated by this idea, we use an existing hand-object interaction detector [11] to find active objects, resulting in a set of bounding boxes. We then use a pre-trained object detector [54] to associate object labels to the detected active objects when their bounding boxes are largely overlapped with intersection over union $\text{IoU} > 0.25$. The set of objects that are directly interacted with by hands could potentially help the model to focus on task-relevant objects and ignore the rest.

Another intuition we have, which may be complementary to the previous idea, is that the next active object likely has already appeared in the video before the moment of interaction. Moreover, the surroundings in the recording may also provide useful context. Therefore, we select a set of visible objects in each frame as (1) the potential candidates for future active objects and (2) the proxy of the surroundings. To do so, we use the CLIP model, which is a pre-trained multimodal language and vision model using contrastive learning, to compute a cosine similarity between the CLIP image embedding of a frame to a list of pre-defined object categories. We keep the highest-scoring k objects as the visible objects for a given frame and set $k = 5$. Now for each frame, we have one verb-noun pair describing the action $a^t = (n^t, v^t) \in \mathcal{A}$, a list of hand-held objects \mathcal{N}_h , where $|\mathcal{N}_h| \geq 0$, and a list of visible objects \mathcal{N}_v , $|\mathcal{N}_v| > 0$. Note that it is not guaranteed that hand-held objects are detected in each frame and it is possible that $|\mathcal{N}_h| = 0$. However, with the ranking-based approach, we can always find visible objects and satisfy the condition that $|\mathcal{N}_v| > 0$. More details are in the supplementary.

Aggregating action context over multiple frames. As one action (e.g. cutting carrots) may span multiple frames, in order to reduce redundancy and have concise context representation, we merge frames of the same action a into one segment via a cross-frame aggregation scheme. For example, a sequence of 50 frames with 20 times $a^1 =$

(washing carrots), and 30 times $a^2 =$ (cutting carrots), is summarized as (a^1, a^2) with a context length of $L = 2$. We aggregate the list of \mathcal{N}_h and \mathcal{N}_v in a similar fashion. The complete action context \mathcal{C}_L , which consists of action descriptions and a list of objects (either \mathcal{N}_h or \mathcal{N}_v), is then fed into our model by concatenating them in chronological order. By aggregating across frames, we capture dominant actions and objects in the past, reduce noise in the generated language summary and cover longer activity timespans. Details on the cross-frame aggregation can be found in the supplementary material.

3.3. TransFusion: Multimodal fusion

Figure 2 shows the architecture of the proposed multimodal TransFusion model. TransFusion employs two different base encoders for language and image input respectively. The input prediction frame f_T is processed by a regular CNN-based visual encoder [21], which outputs a set of multiscale feature maps $\mathcal{F}_V^s(f_T)$, with s indicating the scale. The summary of action context is encoded by a language encoder [38] and outputs $\mathcal{F}_L(\mathcal{C}_L)$. The feature maps belonging to different scale levels from the visual encoder are fused via a joint-attention scheme with the encoded language features. Their output is then processed by a regular feature pyramid network (FPN) before being fed into the Faster R-CNN [39] detector.

Multimodal fusion. For simplicity, we describe the multimodal fusion module for a single input scale s , which we hence omit from notation. A detailed view of a single Transformer Encoder layer together with the input projection stages is illustrated in Figure 3. For the visual modality, we first split the image into a sequence of tokens. More precisely, the visual features $\mathcal{F}_V(f_T) \in \mathbb{R}^{C \times H \times W}$ are reshaped to $\mathbb{R}^{N \times (P^2 \cdot C)}$, where P is the token size and $N = \frac{H \times W}{P^2}$ the number of tokens. We add unique type embeddings to each modality as well as a positional encoding.

Both visual and language tokens are first mapped to \mathbb{R}^D via a linear project and then concatenated together before being fed to the fusion module. The fusion block consists of a regular Transformer encoder layer stacked M times together. In the end, the visual tokens are regrouped into their initial shape to compose the feature map for the feature pyramid network (FPN).

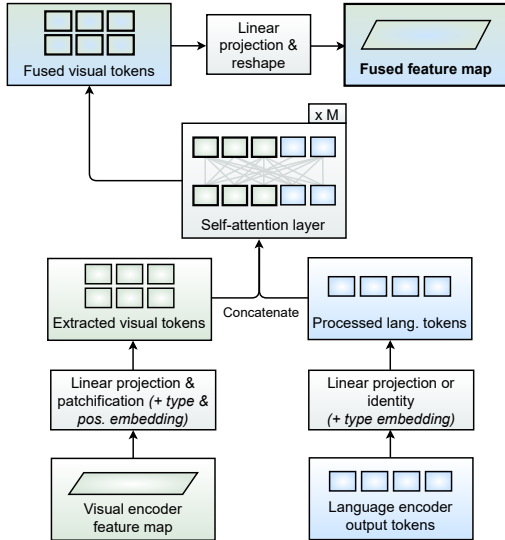


Figure 3. **Multimodal fusion module.** We first project the CNN feature map and the language tokens to a common dimensionality before adding the specific embeddings. We concatenate the visual and language tokens and feed them to M self-attention layers. At the output, we select the fused visual tokens and project them back into the initial shape of the feature map.

Multiscale fusion. The multimodal fusion block outputs multiple feature maps of varying scales, and they are fed into FPN. FPN has different parameters for each feature map, allowing the network to learn specialized features for each downsampling ratio. The output of FPN is processed by a Faster R-CNN detector.

Prediction head networks. The Faster R-CNN detector outputs the bounding box b through a regression layer, an associated object n and verb v , and time to contact t .

Training objective. We train TransFusion using the standard Faster R-CNN [39] objective \mathcal{L}_{box} for bounding box prediction, which consists of the localization and objectness, cross-entropy losses \mathcal{L}_{noun} and \mathcal{L}_{verb} for noun and verb prediction respectively, and an L1 loss \mathcal{L}_{ttc} for time to contact prediction. The overall objective is

$$\mathcal{L} = \mathcal{L}_{box} + \mathcal{L}_{noun} + \mathcal{L}_{verb} + \mathcal{L}_{ttc}. \quad (1)$$

As defined in Faster R-CNN, \mathcal{L}_{box} is

$$\mathcal{L}_{box} = \frac{1}{N_{cls}} \sum_i \mathcal{L}_{cls}(p_i, p_i^*) + \frac{\lambda}{N_{reg}} \sum_i p_i^* \cdot L_{reg}(b_i - b_i^*), \quad (2)$$

where p_i is the predicted probability of a box being classified as a foreground object (true positive), p_i^* is the ground-truth label; b_i and b_i^* are the predicted and ground-truth box coordinates. We set $N_{cls} = 64$ and leave $\lambda = 11$. N_{reg} is the number of bounding boxes used in training.

4. Experiments

Dataset. We use the dataset provided for the short-term object interaction anticipation task in **Ego4D** [20]. It contains various activities ranging from gardening work to cooking or car parts changing. It consists of 64,798 annotated video clips of 5 minutes each with frame rate $fps = 30$. The dataset has highly imbalanced long tail distributions of ground-truth labels including 87 nouns and 74 verbs (e.g. the “take” class is almost 50% of all the verb labels while “mold” appears only in one video). Following Ego4D’s data split, the train set consists of about 28k samples, while the rest are roughly equally split between the validation and the test sets. We also experimented with the EK100 dataset [9] that consists of unscripted, egocentric kitchen activities together with interaction labels for 300 objects and 97 actions.

Evaluation. Following the Ego4D benchmark setting, we use the Top-5 mean Average Precision (mAP) to evaluate the performance of individual predictions. It considers two constraints: The **IoU** constraint requires that the predicted boxes are counted as hits only with intersection over union $IoU \geq 0.5$ with a ground-truth box; the **TTC** constraint requires that the predicted time-to-contact t_i is close enough to the ground-truth \hat{t}_i , i.e. $|t_i - \hat{t}_i| < T_\delta, T_\delta = 0.25$.

- **Noun** refers to the Noun-Box Top-5 mAP. In addition to the IoU constraint, exact matches with the ground-truth nouns are required.
- **Noun-Verb** refers to the Noun-Verb-Box Top-5 mAP. Exact noun and verb matches with the IoU constraint.
- **Noun-TTC** refers to the Noun-Box Top-5 mAP. Exact noun matches with the TTC constraint.
- **Noun-Verb-TTC (“Overall”)** refers to the overall Top-5 mAP, intersecting exact noun-verb matches with IoU and TTC constraints.

Note that as detecting the next-active objects is the main focus of the task, all evaluation metrics are conditioned on the IoU constraint.

Implementation details. For implementation, we make use of the pre-trained Torchvision Faster R-CNN. ResNet-50 [21] is used as the visual encoder and Sentence-BERT (SBERT) [38] is used as the language encoder. We further transfer the ResNet-50 and Faster R-CNN weights from the Ego4D model to further improve the performance of TransFusion. We freeze ResNet-50 and apply the multimodal fusion scheme on top. For the multimodal fusion module, we stack 4 layers of the transformer encoder for each of the FPN input layers with a $4 \times$ feed-forward multiplier and token dropout of 0.2. We use the RAdam [30] optimizer

Set	Model	N \uparrow	N-V \uparrow	N-T \uparrow	A \uparrow
Val	Ego4D [20]	17.55	5.19	5.37	2.07
	TF (ours)	20.19	7.55	6.13	2.60
	Improvement	15.3%	45.4%	10.6%	25.6%
Test	Ego4D [20]	20.45	6.78	6.17	2.45
	TF (ours)	24.69	9.97	7.33	3.44
	Improvement	25.6%	47%	18.8%	40.4%

Table 1. **Comparison to the state-of-the-art on short-term object interaction anticipation.** We report top-5 Noun (N), Noun-Verb (N-V), Noun-TTC (N-T), and Overall (A) on the Ego4D validation (Val) and test (Test) splits. TF is short for TransFusion. We outperform Ego4D by a large margin and the relative improvements are reported in percentage.

with a weight decay of $2e^{-4}$, and an effective batch size of 32. Besides the default Faster R-CNN background class in nouns, we also add it in the verb classes prediction head which improves the Noun-Verb mAP by almost 2 points.

During development, we noted that compared to our visual-only baselines, the multimodal models reach high confidence in predicting foreground objects with a corresponding local minimum of the loss before learning to fuse the visual and language modalities effectively. Hence, we reduced the region proposal network’s sampling batch size and the detection network’s image batch size from 256 and 512 to 64 and 256 respectively, penalizing the model less for foreground-background mismatches. This allows the model to learn a more effective feature fusion and reduces the dependence on the visual features, which are already adapted for object detection tasks. We also perform multiscale augmentation by resizing the shortest edge between 480 and 768 pixels, random-relative cropping, color jittering and image horizontal flipping.

4.1. Comparison with state-of-the-art

We first compare our method against the current state-of-the-art presented in Ego4D [20] on the validation and test sets. The **Ego4D** baseline employs a two-stage approach consisting of a ResNet-based Faster R-CNN detector and a SlowFast [15] 3D CNN video processing module. The Faster R-CNN outputs bounding boxes and noun predictions on the prediction frame, without using any video features. The detected boxes are used to perform region of interest (ROI) pooling [19] on the corresponding SlowFast 3D CNN video features. The pooled video features predict the verb and the time-to-contact values.

We use pre-trained ResNet50 and SBERT 384 as the visual and language encoder respectively. Unless specified otherwise, we use $L_c=3$. As shown in Table 1, our method significantly outperforms the state-of-the-art Ego4D approach. In particular, in terms of the Noun-Verb and Noun-Verb-TTC (“Overall”), TransFusion achieves strong top-5 mAP performance of 7.55 and 2.60 respectively on the val-

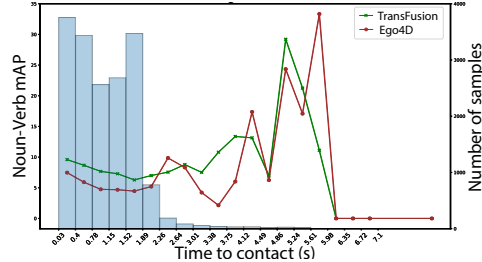


Figure 4. **Prediction of Noun-Verb in relation to time to contact.** Histogram of the time-to-contact labels are shown in blue bars. Performance measured in Noun-Verb is plotted as a function of time to contact, TransFusion in green and Ego4D in red.

idation set, in contrast to Ego4D’s performance of 5.19 and 2.07. TransFusion also achieves a strong performance of 9.97 mAP in Noun-Verb and 3.44 mAP in Overall on the test set, where corresponding Ego4D’s results are 6.78 and 2.45. The relative improvements are 45.4% and 25.6% of Noun-Verb and Overall on the validation set, and 47.0% and 40.4% respectively on the test set. This demonstrates the advantages of modeling action context explicitly for the interaction anticipation task, in addition to the single pass prediction through end-to-end learning.

We observe a noticeable fluctuation in all metrics when moving from the validation set to the test set, hinting towards a difference between the data distributions of the two sets. For the test set we report the model performance obtained by using all the available labeled data from the challenge. Using only the training subset results in lower performance of 8.52 N-V and 2.97 Overall. With the current results we rank 1st in N, N-V (the classification metrics) and 2nd in N-T and Overall on the challenge leaderboard.

Figure 4 shows the long tail distribution of the time-to-contact labels in the validation set. We also see that TransFusion consistently outperforms Ego4D when a sufficient amount of data is available, however, the performance starts to fluctuate when it comes to the long tail part. An additional per-video comparison shows that our model outperforms the baseline model in Noun mAP on all 2930 samples from 81 videos. Their content varies from “playing board games”, “construction jobs”, “farming” and “cooking” which further shows the reliability of our approach. In contrast, the baseline work is superior on only 10 videos.

4.2. Evaluation of generated summary

In Table 2, we compare different variants of generated summary against ground-truth labels (GT) provided by Ego4D, which gives us a reasonable upper bound of the performance. As we expect major differences in semantic-level performance, we report the results only in Noun and Noun-Verb, without using any TTC-related metrics. Experiments using multiple versions of generated summaries show that

Summary	\mathcal{A}	\mathcal{N}_V	$\mathcal{A} + \mathcal{N}_h$	$\mathcal{A} + \mathcal{N}_v$	GT
N \uparrow	18.67	19.62	19.43	19.63	21.71
N-V \uparrow	7.16	7.13	6.71	7.36	7.86

Table 2. **Evaluation of generated summaries.** We evaluate the quality of the generated summaries and compare different variants against ground-truth annotations (GT) provided by the Ego4D dataset. GT only contains action descriptions of verb-noun pairs. Top-5 Noun (N), and Noun-Verb (N-V) are reported.

we achieve results comparable to GT, and adding visible objects to generated verb-noun annotations improves task performance. Note that compared to GT, the generated summaries may have multiple semantically similar descriptions (e.g. “cut carrot” and “cut vegetable”). These taken together offer a reasonable picture of using language summaries to represent action context, although we notice a domain gap in the choice of words between the generated labels and the ground-truth ones. In some cases, even if the description is satisfactory for a human evaluator, the information may be too vague to be directly useful to the model. Phrasing differences between the generated captions and the training corpus of the language encoders can also be a bottleneck.

4.3. Ablation studies

Comparison to video features. We evaluate whether language summary can better represent action context than video frames. To do so, we implement **TransFusion-Video**, which takes video features extracted from the Ego4D SlowFast [15] model as input and uses the identical fusion module as in TransFusion. Given an action segment of one second with 30 frames, language can summarize it in two words whereas corresponding video features can easily take up more than 12 times space (e.g. smaller SBERT [38] feature of 2×384 compared to SlowFast [15] feature of 4×2304). Therefore, using language summary allows us to model considerably longer action context. Besides, the baseline 2nd stage SlowFast model has 33 million parameters and is trained end-to-end in Ego4D while the small SBERT encoder has 22 million parameters and we only finetune the last layer of 1.7 million parameters.

Compared to the best TransFusion performance with $L_c=2$, the best TransFusion-video achieves a decrease of 1.36 in mAP Noun and 0.44 in mAP Verb (18.26 mAP Noun and 6.73 mAP Noun-Verb) when 80 video frames (=2.6s) are used as input. More details can be found in Figure 5. For video features, the domain gap between various datasets seems to be too large to allow effective generalization to a diverse dataset such as Ego4D. We suspect that the feature representations are more entangled due to the need to represent temporal, visual, and semantic scene aspects simultaneously. In contrast, the temporal aspect is directly encoded in the syntax of the summary, i.e. the succession of words.

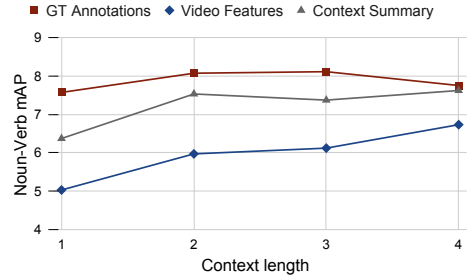


Figure 5. **Context length ablations.** Our method using language summary as input (Context Summary) outperforms the video-features-based approach (Video Features) across different context lengths ranging from one to four, measured by Noun-Verb mAP. TransFusion using GT annotations are plotted as an upper bound.

Visual Encoder	Input Resolution	N \uparrow	N-V \uparrow
ResNet-50	1024×768	19.64	7.17
MobileNetV3	640×480	13.23	4.56
ResNet-50 backbone	1024×768	16.26	5.97

Table 3. **Visual encoder ablations.** We report validation Top-5 Noun (N), and Noun-Verb (N-V) for different visual encoders.

Length of action context. A significant parameter in obtaining good performance is the length of action context, i.e., how many past actions to include in the input. As shown in Figure 5, TransFusion achieves the best overall performance with $L=4$ (mAP=7.62), and a comparable result with $L=2$ (mAP=7.53). We notice that activities that have a more structured nature or certain repeating patterns (such as cooking or repairing a bicycle) are easier to model with an increased context length compared to inherently more random activities (such as playing basketball).

Visual encoder. We experiment using both ResNet-50 [21] and MobileNetV3 [23] visual encoders. The results are reported on the validation set in Table 3. Additionally, we also compare the results when Faster R-CNN is trained from scratch instead of using pre-trained Ego4D weights, labeled as ResNet-50 backbone. TransFusion is able to benefit from large image resolution and pre-trained Ego4D weights.

Language encoder. In order to understand the impact of the choice of language encoders, we also experiment with other LLMs including SBERT with a RoBERTa backbone [32, 38], GPT-2 [36], and FLAN-T5 [8] using the validation set. We finetune the last layer for each of the language encoders from the start of training. Table 4 summarizes the performance of different language encoders, showing that the SBERT models perform best. Note that the models are trained without the time-to-contact prediction. We hypothesize that the difference comes from the training objectives of language models. SBERT is trained by comparing the similarity of two sentences so it can bring the embeddings of semantically similar sentences closer to

Language Encoder	Token size	N \uparrow	N-V \uparrow
SBERT/BERT [13, 38]	384	20.09	7.62
SBERT/roBERTa [32, 38]	768	19.78	7.78
GPT-2 [36]	768	18.98	7.08
Flan-T5 [8]	1024	18.26	6.61

Table 4. **Language encoder ablations.** We compare SBERT using BERT and RoBERTa backbones with different language encoders, GPT-2 and Flan-T5. In the table, we include the original token size output by each language encoder. In this experiment, we project these output tokens to an embedding of dimension 768 before fusion. We report Top-5 Noun (N) and Noun-Verb (N-V).

each other. This is particularly useful when the model needs to understand descriptions that use synonyms or semantically close words, e.g. “cut carrots” and “slice carrots”. In contrast, for the language models that trained with generative objectives (i.e. optimize for next token prediction), like GPT-2 and FLAN-T5, we find they are very sensitive to the input word choice and can produce significantly different outputs when the input differs by a single punctuation mark.

Alternative multimodal fusion weights. We also compare two versions of the fusion module: with and without shared weights between the Transformer encoder layers. The model with shared weights has a strong regularizing effect while the other converges faster and benefits more from Faster R-CNN pre-trained weights.

Multiscale fusion stages. We ablate the number of fusion stages in TransFusion using MobileNet as the visual encoder. Compared to the two stages in FPN, adding a third FPN stage to the visual encoder provided a boost of 0.4 mAP Noun and 0.7 mAP if we only evaluate the predicted bounding boxes using the IoU constraint.

4.4. Generalizability

To understand if our proposed model generalizes to other videos, we further test our model on the EK100 [9] dataset. Since EK100 consists of unscripted cooking activities performed by different actors, we can assess if our model is capable of picking up action regularities across different types of actors. We also split the EK100 dataset such that the model does not see the clips from the same video at train and validation, whereas in Ego4d, the model may encounter this. Under this setting, the model needs to learn video/actor-specific cues while not overfitting to them. Each video is preprocessed to obtain the ground-truth labels by matching UniDet [54] object detection classes to the subsequent action recognition labels. We set an initial Δ to be 0.4s for each action and progressively increase Δ until we find a matching pair. Since UniDet produces noisier detection for finer-grain categories, in order to get reliable NAO labels, we choose to merge similar classes together. We re-

Model	N \uparrow	N-V \uparrow
TransFusion GT	6.47	2.58
TransFusion Summary	4.26	1.63
TransFusion-Video	4.02	1.66

Table 5. **Object interaction anticipation on EK100.** EK100 results using generated ground-truth (GT), generated summary, and video features. We report Top-5 Noun (N) and Noun-Verb (N-V).

duce the number of nouns from 300 to 88 and the number of verbs from 97 to 66 by merging similar classes, e.g. combining “salt”, “pepper”, and “chilli flakes” into “seasoning”. This preserves the semantics of classes without significantly lowering the difficulty of the problem. Compared to Ego4d which has a single vegetable-fruit class, EK100 has a richer set of nouns for vegetables and fruits including “salad”, “parsley”, “bean”, “tomato”, etc. We then train our models with Ego4d pretrained Faster R-CNN on EK100.

Table 5 compares the results of models trained with the preprocessed ground-truth labels, generated summary, and video features. It suggests that TransFusion learns to represent structured activities effectively with the inclusion of language features. Compared with the video features, the context represented by generated summary shows an improvement of mAP Noun and a similar performance of mAP Verb which matches our results in Ego4D.

5. Conclusion and discussion

We propose a multimodal fusion model, TransFusion, that anticipates object interactions by considering past action context represented by language summaries. Our experiments on two challenging egocentric video datasets demonstrate how language summaries can improve object interaction anticipation, highlighting the representational power of concise language descriptions.

While we do not consider any temporal information, it is possible to integrate motion cues like optical flow to improve the prediction of time to contact.

We would like to highlight that the proposed approach is not limited to object interaction anticipation. In general, language provides a universal interface to complement the visual input with information encoded in language models or task-specific pipelines.

Future work can leverage language summary for other video reasoning tasks [52, 53], or extend it to describe the possible future activities [1, 28] for long-term interaction anticipation.

Acknowledge This work was supported by an ETH Zurich Postdoctoral Fellowship. We thank Velko Vechev for the voice-over.

References

- [1] Chaitanya Ahuja and Louis-Philippe Morency. Language2pose: Natural language grounded pose forecasting. In *2019 International Conference on 3D Vision (3DV)*, pages 719–728, 2019. 8
- [2] Alan Akbik, Duncan Blythe, and Roland Vollgraf. Contextual string embeddings for sequence labeling. In *Proceedings of the 27th international conference on computational linguistics*, pages 1638–1649, 2018. 3, 12
- [3] Stanislaw Antol, Aishwarya Agrawal, Jiasen Lu, Margaret Mitchell, Dhruv Batra, C Lawrence Zitnick, and Devi Parikh. Vqa: Visual question answering. In *Proceedings of the IEEE international conference on computer vision*, pages 2425–2433, 2015. 3
- [4] Jimmy Lei Ba, Jamie Ryan Kiros, and Geoffrey E. Hinton. Layer normalization, 2016. 13
- [5] Max Bain, Arsha Nagrani, Gül Varol, and Andrew Zisserman. Frozen in time: A joint video and image encoder for end-to-end retrieval. *CoRR*, abs/2104.00650, 2021. 3
- [6] Gedas Bertasius, Hyun Soo Park, Stella X. Yu, and Jianbo Shi. First-person action-object detection with egonet. In *Proceedings of Robotics: Science and Systems*, July 2017. 2
- [7] Jerome S Bruner. Intention in the structure of action and interaction. *Advances in infancy research*, 1981. 2
- [8] Hyung Won Chung, Le Hou, Shayne Longpre, Barret Zoph, Yi Tay, William Fedus, Eric Li, Xuezhi Wang, Mostafa Dehghani, Siddhartha Brahma, Albert Webson, Shixiang Shane Gu, Zhuyun Dai, Mirac Suzgun, Xinyun Chen, Aakanksha Chowdhery, Sharan Narang, Gaurav Mishra, Adams Yu, Vincent Zhao, Yanping Huang, Andrew Dai, Hongkun Yu, Slav Petrov, Ed H. Chi, Jeff Dean, Jacob Devlin, Adam Roberts, Denny Zhou, Quoc V. Le, and Jason Wei. Scaling instruction-finetuned language models, 2022. 3, 7, 8
- [9] Dima Damen, Hazel Doughty, Giovanni Maria Farinella, Antonino Furnari, Evangelos Kazakos, Jian Ma, Davide Moltisanti, Jonathan Munro, Toby Perrett, Will Price, et al. Rescaling egocentric vision: collection, pipeline and challenges for epic-kitchens-100. *International Journal of Computer Vision*, 130(1):33–55, 2022. 2, 3, 5, 8
- [10] Dima Damen, Hazel Doughty, Giovanni Maria Farinella, Antonino Furnari, Evangelos Kazakos, Jian Ma, Davide Moltisanti, Jonathan Munro, Toby Perrett, Will Price, and Michael Wray. Rescaling egocentric vision. *CoRR*, abs/2006.13256, 2020. 3
- [11] Ahmad Darkhalil, Dandan Shan, Bin Zhu, Jian Ma, Amlan Kar, Richard Higgins, Sanja Fidler, David Fouhey, and Dima Damen. Epic-kitchens visor benchmark: Video segmentations and object relations. In *Proceedings of the Neural Information Processing Systems (NeurIPS) Track on Datasets and Benchmarks*, 2022. 4
- [12] Jiajun Deng, Zhengyuan Yang, Tianlang Chen, Wengang Zhou, and Houqiang Li. Transvg: End-to-end visual grounding with transformers. *CoRR*, abs/2104.08541, 2021. 3
- [13] Jacob Devlin, Ming-Wei Chang, Kenton Lee, and Kristina Toutanova. BERT: pre-training of deep bidirectional transformers for language understanding. *CoRR*, abs/1810.04805, 2018. 3, 8
- [14] Alexey Dosovitskiy, Lucas Beyer, Alexander Kolesnikov, Dirk Weissenborn, Xiaohua Zhai, Thomas Unterthiner, Mostafa Dehghani, Matthias Minderer, Georg Heigold, Sylvain Gelly, Jakob Uszkoreit, and Neil Houlsby. An image is worth 16x16 words: Transformers for image recognition at scale. *CoRR*, abs/2010.11929, 2020. 3
- [15] Christoph Feichtenhofer, Haoqi Fan, Jitendra Malik, and Kaiming He. Slowfast networks for video recognition. *CoRR*, abs/1812.03982, 2018. 6, 7
- [16] Antonino Furnari, Sebastiano Battiato, Kristen Grauman, and Giovanni Maria Farinella. Next-active-object prediction from egocentric videos. *CoRR*, abs/1904.05250, 2019. 1, 2
- [17] Antonino Furnari and Giovanni Maria Farinella. Rolling-unrolling lstms for action anticipation from first-person video. *CoRR*, abs/2005.02190, 2020. 3
- [18] Rohit Girdhar and Kristen Grauman. Anticipative Video Transformer. In *ICCV*, 2021. 3
- [19] Ross B. Girshick. Fast R-CNN. *CoRR*, abs/1504.08083, 2015. 6
- [20] Kristen Grauman, Andrew Westbury, Eugene Byrne, Zachary Chavis, Antonino Furnari, Rohit Girdhar, Jackson Hamburger, Hao Jiang, Miao Liu, Xingyu Liu, Miguel Martin, Tushar Nagarajan, Ilija Radosavovic, Santhosh Kumar Ramakrishnan, Fiona Ryan, Jayant Sharma, Michael Wray, Mengmeng Xu, Eric Zhongcong Xu, Chen Zhao, Siddhant Bansal, Dhruv Batra, Vincent Cartillier, Sean Crane, Tien Do, Morrie Doulaty, Akshay Erapalli, Christoph Feichtenhofer, Adriano Fragomeni, Qichen Fu, Christian Fuegen, Abrahm Gebreselasie, Cristina Gonzalez, James Hillis, Xuhua Huang, Yifei Huang, Wenqi Jia, Weslie Khoo, Jachym Kolar, Satwik Kottur, Anurag Kumar, Federico Landini, Chao Li, Yanghao Li, Zhenqiang Li, Karttikeya Mangalam, Raghava Modhugu, Jonathan Munro, Tullie Murrell, Takumi Nishiyasu, Will Price, Paola Ruiz Puentes, Mery Ramazanov, Leda Sari, Kiran Somasundaram, Audrey Southerland, Yusuke Sugano, Ruijie Tao, Minh Vo, Yuchen Wang, Xindi Wu, Takuma Yagi, Yunyi Zhu, Pablo Arbelaez, David Crandall, Dima Damen, Giovanni Maria Farinella, Bernard Ghanem, Vamsi Krishna Ithapu, C. V. Jawahar, Hanbyul Joo, Kris Kitani, Haizhou Li, Richard Newcombe, Aude Oliva, Hyun Soo Park, James M. Rehg, Yoichi Sato, Jianbo Shi, Mike Zheng Shou, Antonio Torralba, Lorenzo Torresani, Mingfei Yan, and Jitendra Malik. Ego4d: Around the World in 3,000 Hours of Egocentric Video. *CoRR*, abs/2110.07058, 2021. 1, 2, 3, 5, 6
- [21] Kaiming He, Xiangyu Zhang, Shaoqing Ren, and Jian Sun. Deep residual learning for image recognition. *CoRR*, abs/1512.03385, 2015. 4, 5, 7
- [22] Dan Hendrycks and Kevin Gimpel. Bridging nonlinearities and stochastic regularizers with gaussian error linear units. *CoRR*, abs/1606.08415, 2016. 13
- [23] Andrew Howard, Mark Sandler, Grace Chu, Liang-Chieh Chen, Bo Chen, Mingxing Tan, Weijun Wang, Yukun Zhu, Ruoming Pang, Vijay Vasudevan, Quoc V. Le, and Hartwig Adam. Searching for mobilenetv3. *CoRR*, abs/1905.02244, 2019. 7

- [24] Zhicheng Huang, Zhaoyang Zeng, Bei Liu, Dongmei Fu, and Jianlong Fu. Pixel-bert: Aligning image pixels with text by deep multi-modal transformers. *CoRR*, abs/2004.00849, 2020. 3
- [25] Will Kay, João Carreira, Karen Simonyan, Brian Zhang, Chloe Hillier, Sudheendra Vijayanarasimhan, Fabio Viola, Tim Green, Trevor Back, Paul Natsev, Mustafa Suleyman, and Andrew Zisserman. The kinetics human action video dataset. *CoRR*, abs/1705.06950, 2017. 17
- [26] Evangelos Kazakos, Arsha Nagrani, Andrew Zisserman, and Dima Damen. Epic-fusion: Audio-visual temporal binding for egocentric action recognition. *CoRR*, abs/1908.08498, 2019. 3
- [27] Weicheng Kuo, Fred Bertsch, Wei Li, AJ Piergiovanni, Mohammad Saffar, and Anelia Angelova. Findit: Generalized localization with natural language queries, 2022. 3
- [28] Yen-Ling Kuo, Xin Huang, Andrei Barbu, Stephen G McGill, Boris Katz, John J Leonard, and Guy Rosman. Trajectory prediction with linguistic representations. In *2022 International Conference on Robotics and Automation (ICRA)*, pages 2868–2875. IEEE, 2022. 8
- [29] Jie Lei, Linjie Li, Luowei Zhou, Zhe Gan, Tamara L. Berg, Mohit Bansal, and Jingjing Liu. Less is more: Clipbert for video-and-language learning via sparse sampling. *CoRR*, abs/2102.06183, 2021. 3
- [30] Liyuan Liu, Haoming Jiang, Pengcheng He, Weizhu Chen, Xiaodong Liu, Jianfeng Gao, and Jiawei Han. On the variance of the adaptive learning rate and beyond. *CoRR*, abs/1908.03265, 2019. 5
- [31] Miao Liu, Siyu Tang, Yin Li, and James M. Rehg. Forecasting human object interaction: Joint prediction of motor attention and egocentric activity. *CoRR*, abs/1911.10967, 2019. 2
- [32] Yinhan Liu, Mylène Ott, Naman Goyal, Jingfei Du, Mandar Joshi, Danqi Chen, Omer Levy, Mike Lewis, Luke Zettlemoyer, and Veselin Stoyanov. Roberta: A robustly optimized BERT pretraining approach. *CoRR*, abs/1907.11692, 2019. 7, 8
- [33] David W Orr. *The nature of design: ecology, culture, and human intention*. Oxford University Press, 2002. 2
- [34] Jeffrey Pennington, Richard Socher, and Christopher Manning. GloVe: Global vectors for word representation. In *Proceedings of the 2014 Conference on Empirical Methods in Natural Language Processing (EMNLP)*, pages 1532–1543, Doha, Qatar, Oct. 2014. Association for Computational Linguistics. 18
- [35] Alec Radford, Jong Wook Kim, Chris Hallacy, Aditya Ramesh, Gabriel Goh, Sandhini Agarwal, Girish Sastry, Amanda Askell, Pamela Mishkin, Jack Clark, Gretchen Krueger, and Ilya Sutskever. Learning transferable visual models from natural language supervision. *CoRR*, abs/2103.00020, 2021. 2, 3
- [36] Alec Radford, Jeff Wu, Rewon Child, David Luan, Dario Amodei, and Ilya Sutskever. Language models are unsupervised multitask learners. 2019. 3, 7, 8
- [37] Colin Raffel, Noam Shazeer, Adam Roberts, Katherine Lee, Sharan Narang, Michael Matena, Yanqi Zhou, Wei Li, and Peter J. Liu. Exploring the limits of transfer learning with a unified text-to-text transformer. *CoRR*, abs/1910.10683, 2019. 3
- [38] Nils Reimers and Iryna Gurevych. Sentence-bert: Sentence embeddings using siamese bert-networks. *CoRR*, abs/1908.10084, 2019. 3, 4, 5, 7, 8
- [39] Shaoqing Ren, Kaiming He, Ross B. Girshick, and Jian Sun. Faster R-CNN: towards real-time object detection with region proposal networks. *CoRR*, abs/1506.01497, 2015. 4, 5
- [40] Paschal Sheeran. Intention—behavior relations: a conceptual and empirical review. *European review of social psychology*, 12(1):1–36, 2002. 2
- [41] Nitish Srivastava, Geoffrey Hinton, Alex Krizhevsky, Ilya Sutskever, and Ruslan Salakhutdinov. Dropout: A simple way to prevent neural networks from overfitting. *Journal of Machine Learning Research*, 15(56):1929–1958, 2014. 13
- [42] Chen Sun, Fabien Baradel, Kevin Murphy, and Cordelia Schmid. Contrastive bidirectional transformer for temporal representation learning. *CoRR*, abs/1906.05743, 2019. 3
- [43] Hao Tan and Mohit Bansal. LXMERT: learning cross-modality encoder representations from transformers. *CoRR*, abs/1908.07490, 2019. 3
- [44] Laurens van der Maaten and Geoffrey Hinton. Visualizing data using t-sne. *Journal of Machine Learning Research*, 9(86):2579–2605, 2008. 18
- [45] Ashish Vaswani, Noam Shazeer, Niki Parmar, Jakob Uszkoreit, Llion Jones, Aidan N. Gomez, Lukasz Kaiser, and Illia Polosukhin. Attention is all you need. *CoRR*, abs/1706.03762, 2017. 13
- [46] Peng Wang, An Yang, Rui Men, Junyang Lin, Shuai Bai, Zhikang Li, Jianxin Ma, Chang Zhou, Jingren Zhou, and Hongxia Yang. Ofa: Unifying architectures, tasks, and modalities through a simple sequence-to-sequence learning framework. *CoRR*, abs/2202.03052, 2022. 3, 12
- [47] Chao-Yuan Wu, Yanghao Li, Karttikeya Mangalam, Haoqi Fan, Bo Xiong, Jitendra Malik, and Christoph Feichtenhofer. Memvit: Memory-augmented multiscale vision transformer for efficient long-term video recognition. *CoRR*, abs/2201.08383, 2022. 3
- [48] Yu Wu, Linchao Zhu, Xiaohan Wang, Yi Yang, and Fei Wu. Learning to anticipate egocentric actions by imagination. *CoRR*, abs/2101.04924, 2021. 3
- [49] Kelvin Xu, Jimmy Ba, Ryan Kiros, Kyunghyun Cho, Aaron Courville, Ruslan Salakhudinov, Rich Zemel, and Yoshua Bengio. Show, attend and tell: Neural image caption generation with visual attention. In *International conference on machine learning*, pages 2048–2057. PMLR, 2015. 3
- [50] Ting Yao, Yingwei Pan, Yehao Li, Zhaofan Qiu, and Tao Mei. Boosting image captioning with attributes. In *Proceedings of the IEEE international conference on computer vision*, pages 4894–4902, 2017. 3
- [51] Rowan Zellers, Ximing Lu, Jack Hessel, Youngjae Yu, Jae Sung Park, Jize Cao, Ali Farhadi, and Yejin Choi. MERLOT: multimodal neural script knowledge models. *CoRR*, abs/2106.02636, 2021. 3
- [52] Kuo-Hao Zeng, Tseng-Hung Chen, Ching-Yao Chuang, Yuan-Hong Liao, Juan Carlos Niebles, and Min Sun. Leveraging video descriptions to learn video question answering.

In *Thirty-First AAAI Conference on Artificial Intelligence*, 2017. 8

[53] Ke Zhang, Wei-Lun Chao, Fei Sha, and Kristen Grauman. Video summarization with long short-term memory. In *European conference on computer vision*, pages 766–782. Springer, 2016. 8

[54] Xingyi Zhou, Vladlen Koltun, and Philipp Krähenbühl. Simple multi-dataset detection. *CoRR*, abs/2102.13086, 2021. 4, 8

Summarize the Past to Predict the Future: Natural Language Descriptions of Context Boost Multimodal Object Interaction Anticipation

[Supplementary Material]

6. Past summarization

Extracting verb-noun action pairs We use the task-agnostic and modality-agnostic OFA model [46] to generate captions for each frame of interest. Multiple image captions (e.g. “a person cutting vegetables”) are first generated by diverse prompts to OFA. The prompts used are “what does the image describe?”, “what is the person in this picture doing?”, and “what is happening in this picture?”

We then perform part-of-speech tagging on the prose captions using Flair [2] to extract the verb-noun pairs (e.g. “cut vegetable”) representing the action context, and use the majority-based selection strategy described in Section 3.2 of the main paper to obtain at most one verb-noun pair per processed frame.

Aggregating action context across frames For a given frame on which to predict, we mark the 150 (Ego4D) resp. 120 (EPIC-KITCHENS) previous frames to be processed by the context extraction models using a stride of 3 frames. The videos in the Ego4D dataset use 30 FPS, while for EPIC-KITCHENS we subsample the videos to 24 FPS. We thus process the preceding 5 seconds for each prediction frame in both datasets. Yet, it is possible for a prediction frame to make use of language context obtained from more than 5 seconds in the past through the inclusion of language context computed for previous prediction frames.

After processing the individual frames, we separately post-process each action context category $c \in \{\mathcal{A}, \mathcal{N}_h, \mathcal{N}_v\}$ (noun-verb pairs, held objects, and visible objects) via a cross-frame aggregation scheme to merge consecutive frames with identical terms into segments. Note how working with language summaries allows us to opt for this simple duplicate elimination scheme, whereas video input is often repetitive and not straightforward to deduplicate.

More specifically, a series of occurrences of a term $v \in \mathcal{V}_c$ in a sequence of frames that is at least $P_{o,c}$ long, with consecutive occurrences at most $P_{\ell,c}$ frames apart, start a new segment. The segment ends once v has not occurred in the last $P_{\ell,c}$ frames. \mathcal{V}_c represents the vocabulary of c , to be explained shortly. For a given context length L_c , we construct an action context of at most L_c non-overlapping

Model	Filtering	NO \uparrow	N \uparrow	N-V \uparrow
$\mathcal{A} + \mathcal{N}_v$	✓	33.20	19.63	7.36
$\mathcal{A} + \mathcal{N}_v$	-	32.38	19.27	7.20
\mathcal{A}	✓	32.41	18.67	7.16
\mathcal{A}	-	30.82	18.05	6.61

Table 6. **Evaluation of filtering of extracted verb-noun action labels.** We evaluate the performance obtained on the Ego4D validation set when training using filtered verb-noun pairs with nouns restricted to the Ego4D noun domain, and when using unfiltered verb-noun pairs. The results show that the filtered versions achieve better performance scores than their unfiltered counterparts.

active and/or past segments, with segments containing more occurrences of their respective term eliminating overlapping segments of different terms with fewer occurrences.

To construct the action context for a given prediction frame and action context category c , we distinguish between the *current* context, and the *past* context, with a context length of L_c resulting in 1 current and $L_c - 1$ past segments for \mathcal{A} and \mathcal{N}_h . For \mathcal{N}_v , we do not consider past segments. Instead, we operate only using currently active segments, as visible objects change quickly throughout video frames and we are interested in summarizing the *recent* environment of the actor for this action context category.

We set $P_{o,\mathcal{A}} = 1$, $P_{o,\mathcal{N}_h} = 7$, $P_{o,\mathcal{N}_v} = 10$. We further use $P_{\ell,\mathcal{A}} = P_{\ell,\mathcal{N}_h} = P_{\ell,\mathcal{N}_v} = 7$. For the experiments in Table 1, $L_{\mathcal{A}} = 3$. For those in Table 2, Table 7 and Table 8, $L_{\mathcal{A}} = 4$. In all cases, $L_{\mathcal{N}_h} = L_{\mathcal{N}_v} = 3$.

Action context vocabularies For the verb-noun action label pairs \mathcal{A} , we have the vocabulary $V_{\mathcal{A}} = V_{\mathcal{A},verb} \times V_{\mathcal{A},noun}$. We restrict $V_{\mathcal{A},noun}$ and $V_{\mathcal{N}_v}$ to the domain of the 87 noun classes used in the Ego4D dataset by eliminating all verb-noun pairs with nouns outside this domain during the cross-frame aggregation. As seen in Table 6, restricting $V_{\mathcal{A},noun}$ in this manner yields better performance for both \mathcal{A} and $\mathcal{A} + \mathcal{N}_v$ models. We hypothesize that using a broad vocabulary might inhibit the model’s ability to learn regularities in the language input, given the limited number of training samples available.

$V_{\mathcal{N}_h}$ is the domain of UniDet object classes, while $V_{\mathcal{A},verb}$ consists of the lemmatized versions of all verbs in the output domain of OFA.

7. The TransFusion model

The fusion module is based on the query-key-value (QKV) attention mechanism popularized by the Transformer [45] architecture. Such an attention aggregation scheme can loosely be interpreted as computing a weighted average of the value vectors v for each of the query vectors, where the weight is given by the compatibility between the query and key vectors: q and k . The final compatibility score is obtained after applying softmax on the pairwise dot products as described in Equation 3.

$$Attention(Q, K, V) = softmax\left(\frac{QK^T}{\sqrt{d_k}}\right)V \quad (3)$$

This attention mechanism is applied multiple times in parallel through a set of attention heads, each one with a distinct set of parameters, such that the attention mechanism is allowed to focus on different input subspaces. The output is finally concatenated and projected to the initial token dimension. The multihead functionality is laid out in Equations 4 and 5.

$$MultiHead(Z) = Concat(head_1, \dots, head_h)W^O \quad (4)$$

$$head_i = Attention(QW_i^Z, KW_i^Z, VW_i^Z) \quad (5)$$

In the following, we state the equations for the visual and language features' tokenization and projection, embedding addition, and concatenation operations prior to feeding the result to the TransFusion module for a single scale level.

$$Vf = patchify(Vf_i) \in \mathbb{R}^{N \times P^2 \cdot c} \quad (6)$$

$$Vf = VfW_p; W_p \in \mathbb{R}^{P^2 \cdot c \times D} \quad (7)$$

$$Lf = LM(X); lf \in \mathbb{R}^{L_A \times D} \quad (8)$$

$$Vf += Vf_{emb} + Pos_{emb} \quad (9)$$

$$Lf = Lf + Lf_{emb} \quad (10)$$

$$Lf = Dropout(Lf) \quad (11)$$

$$Vf = Dropout(Vf) \quad (12)$$

$$Z = Concat(Vf, Lf) \quad (13)$$

where $Vf_{emb} \in \mathbb{R}^D$, $Pos_{emb} \in \mathbb{R}^{N \times D}$, Lf represent the tokenized language features and Vf represent the tokenized visual features.

As described in Section 3, the TransFusion model consists of multiple transformer encoder layers applied in succession. This mechanism is replicated on multiple input scales to enhance the corresponding visual features. A single transformer encoder layer employs Layer Normalization

[4], MLP blocks, multihead QKV self-attention, a Dropout module [41], and the GELU [22] non-linearity. The functioning is described in equation 14, where we drop the scale level indices for simplicity.

$$\begin{aligned} Z' &= LN(MultiHead(Dropout(Z)) + Z) \\ Z' &= MLP(Dropout(GELU(Z'))) + Z' \\ Z' &= LN(Z') \end{aligned} \quad (14)$$

8. Implementation details

For the majority of our runs, we use a learning rate of 1e-4. For training the backbone encoders, we additionally decay the learning rate by 5 to better synchronize with the fusion module dynamics that start from a random initialization.

We augment the data by altering both height and width resolutions while ensuring their downsampled shapes are divisible by the patch sizes. The following height-width pairs are used for most of the experiments: 480-596, 544-640, 640-768, 704-896, 768-896. Before rescaling the images, they are cropped randomly in a relative range of 0.9 for both height and width. This way, we preserve about 80% of the original visual area and reduce the chances of evicting GT boxes. The images are flipped horizontally with a probability of 50%. We apply a moderate amount of color jittering: we alter the brightness in a relative range of $[-0.15, 0.15]$, the contrast in $[-0.1, 0.1]$, and the hue in $[-0.05, 0.05]$.

We use a 1D sinusoidal positional embedding for the visual tokens. The patch dimensions used per level are the following: high-resolution ResNet-50 runs use patch projection sizes of 4, 4, 2, 1 for the FPN stages while the low-resolution MobileNetv3 runs use 2, 1, 1. Smaller patches tend to give better performance, but increase the computational cost of the self-attention mechanism that scales with the square of the number of tokens. We also apply 0.1 – 0.2 (depending on the language model size) language token dropout and 0.1 visual token dropout before the transformer fusion layers, which slightly improves validation performance. Each of our models is trained on a single NVIDIA A100 GPU with 80GB of VRAM.

9. Evaluation of action contexts

Correlation of model performance with language input

Table 2 provides a high-level comparison of the performance obtained using different types of action context language input. In Table 7, we further experiment with providing our models trained on $\mathcal{A} + \mathcal{N}_v$ and \mathcal{N}_v different types of action context during inference. Specifically, we compare between (1) using the original action context class(es) each model was trained with as language input, (2) using the object to be interacted with next, taken from the ground-truth

Lang. used during training	Lang. used during inference	NO \uparrow	VO \uparrow	N \uparrow	N-V \uparrow
$\mathcal{A} + \mathcal{N}_v$	next active obj. (GT)	37.40	11.65	21.86	8.05
$\mathcal{A} + \mathcal{N}_v$	$\mathcal{A} + \mathcal{N}_v$	33.20	12.00	19.63	7.36
$\mathcal{A} + \mathcal{N}_v$	\emptyset	29.51	10.72	17.49	6.46
\mathcal{N}_v	next active obj. (GT)	35.42	9.24	20.78	7.33
\mathcal{N}_v	\mathcal{N}_v	33.33	10.61	19.62	7.13
\mathcal{N}_v	\emptyset	29.73	8.65	17.83	6.18
\emptyset	\emptyset	31.26	10.64	17.71	6.14

Table 7. **Performance of various action context combinations at train and inference time.** Comparison of performance obtained on the Ego4D validation set with models trained on \mathcal{A} and $\mathcal{A} + \mathcal{N}_v$, as well as a visual-only model. For the language-aided models, we experiment with forwarding the ground-truth next active object labels, passing the intended action context to the model, and using no language input (\emptyset). Experimental results show that having the ground-truth NAO labels can further improve the model performance, and that our language-aided model performs competitively to a visual-only version.

	\mathcal{A}	\mathcal{N}_h	\mathcal{N}_V	$\mathcal{A} + \mathcal{N}_h$	$\mathcal{A} + \mathcal{N}_v$	GT
Abs.	4,662	1,119	5,390	5,184	7,484	11,576
Rel.	27.0%	6.49%	31.3%	30.1%	43.5%	67.2%
NO	32.41	31.16	33.33	32.72	33.20	37.33
NO ⁺	41.31	47.42	44.24	40.60	44.60	43.71
NO ⁻	30.52	30.97	31.09	31.60	31.22	30.78

Table 8. **Performance analysis based on the occurrence of next active object labels in language context.** Absolute (Abs.) and relative (Rel.) frequency of the occurrence of the ground-truth next active object class in different types of action context on the Ego4D validation set, together with the performance of models trained on these action context types. Performance is measured in terms of Noun-Only mAP and separately for the full validation set (NO), the subset where the ground-truth next active object class appears in the language summary (NO⁺), and the subset where it does not (NO⁻). The results show the benefit of the next active object appearing in the language input.

labels, as language input, and (3) an ablation where we omit all language input.

Ideally, our models trained with \mathcal{N}_v and $\mathcal{A} + \mathcal{N}_v$ input should be able to make use of salient visible objects enumerated in the language input to better disambiguate between multiple possible next active objects (NAOs). The ground-truth NAO forms a reasonable “best-case” version of the \mathcal{N}_v inputs: we would expect an increase in the models’ performance if the NAO is highlighted to the model as the only salient visible object in the prediction frame. Indeed, as evidenced in Table 7, both the model trained on \mathcal{N}_v and that trained on $\mathcal{A} + \mathcal{N}_v$ perform better when receiving the ground-truth NAO as input, than when receiving the visible objects \mathcal{N}_v from the context generation models. On the other hand, the performance drops when the models do not receive any language input. We would like to point out that the performance of the language-aided models does not suffer significantly when omitting language input, suggesting that the models learn to benefit from the provided action context rather than becoming dependent on it.

We further conduct a comparison of our models’ performance on samples for which the ground-truth NAO appears in the generated language input against that on samples for which it does not and calculate the absolute and relative frequencies of the ground-truth NAO’s appearance. We showcase the results in Table 8. The aforementioned considera-

tions strongly suggest that the models benefit from the \mathcal{N}_v action context due to its ability to highlight salient visible objects in the actor’s environment.

Counterfactual analysis We showcase how changing the action context alters the predictions of the model on various prediction frames from the Ego4D dataset’s validation set. Figure 6 together with Figure 11 illustrate the difference in the predictions of an \mathcal{N}_v -trained model when using language input consisting of the ground-truth class name (left column), compared to using the class name of another object in the image or a similar-looking object (right column). We visualize the top 4 highest-scoring bounding boxes, along with the bounding box capturing the ground-truth next active object (in green) and the language input to the model, visible on the bottom left of the images. The visualizations indicate qualitatively that TransFusion learns to effectively condition its predictions on action context encoded as language summaries to anticipate future object interactions.

10. Comparison with state-of-the-art

In this section, we provide more details on the experiment setup reported in the main paper. For the results presented in Table 1, compared to the parameters from Section

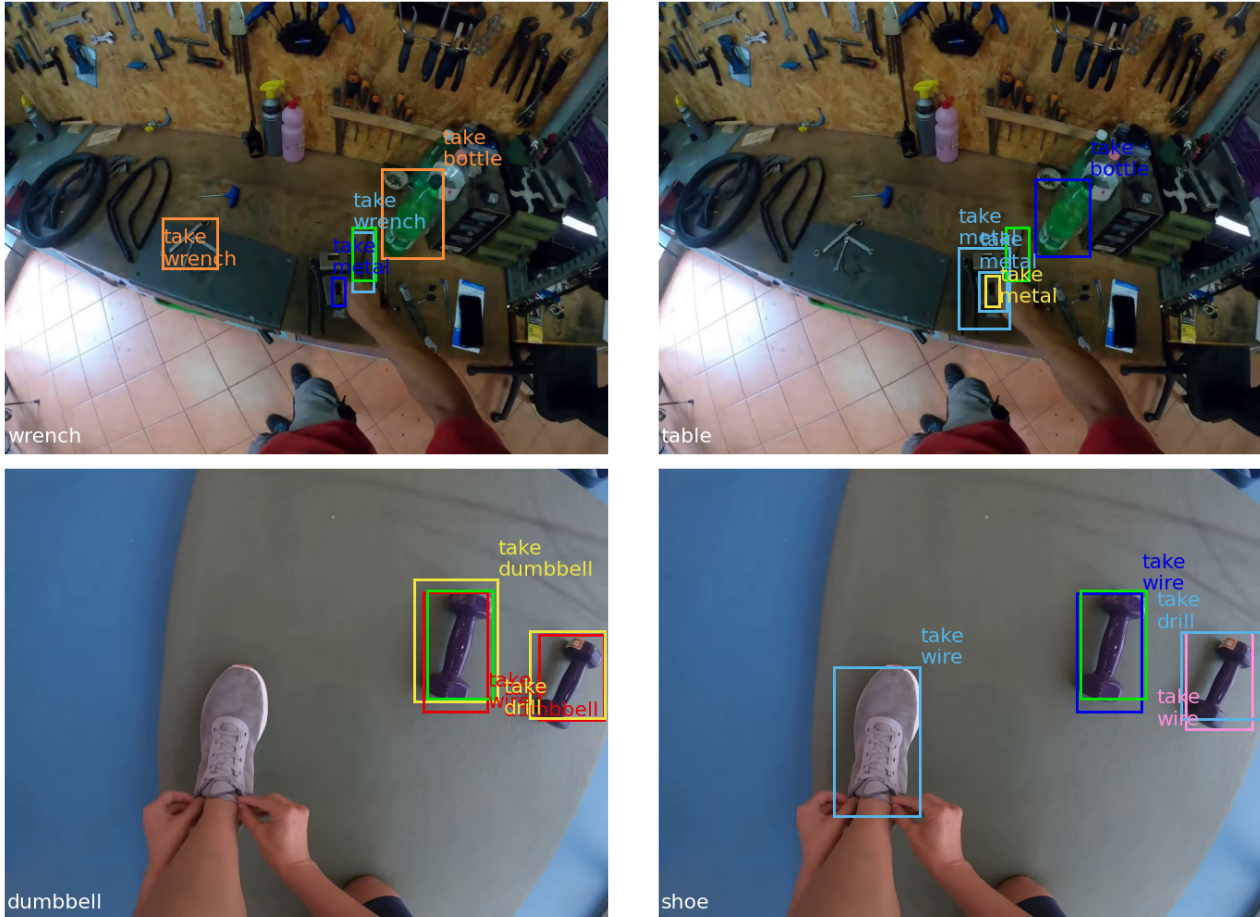


Figure 6. We show the changes in our model’s predictions when altering the language input from *wrench* to *table* on the top row, and *dumbbell* to *shoe* on the bottom row. Additional, similar visualizations are available in Figure 11.

4, we additionally use a step learning rate decay by 0.25 at epoch 6 and an additional input image scale augmentation level of 800-1024 which further boosts the localization performance. For reference, Ego4D resizes the image height to 800 pixels while limiting the width to 1333 pixels. By the choice of height and width ratios, both approaches also provide a weak form of aspect ratio augmentation. The TTC values are obtained using the provided Ego4D model checkpoint while keeping our original box, noun, and verb predictions. For the language encoder, we use SBERT 384 and for the visual encoder, we use the frozen Ego4D ResNet-50 weights. We discount the classification loss for the background class prediction by 0.8 such that the model focuses more capacity on the actual Ego4D categories.

Validation-test performance variance We observe some noticeable variance between the validation and test set performance, both for our model and the Ego4D method. We believe that this is caused by multiple factors, such as 1)

only one validation fold being used during the training of the two models. Performing k -fold cross-validation provides a more reliable estimate of the *true* model performance, at the cost of a significantly larger computation time. 2) even when using a single validation fold, a reasonable performance estimate can be obtained. In our case, we identify a noticeable class distribution shift when moving from the training to the validation set. It is plausible that a similar distribution shift occurs between the validation and test set.

10.1. Additional comparisons

We provide additional insights on how our method performs compared to that of Ego4D, highlighting the effectiveness of our approach and the suitability of using language descriptions to summarize the action context.

Model performance as a function of label distribution

We evaluate the performance of the two models separately for the most frequent and for the tail class categories. This

comparison confirms the effectiveness of our method: we register consistent improvements for both frequent and rare categories: over 15% and 22% for nouns and 132%, 161% for verbs respectively. This is very encouraging, seeing as improving performance in low-tail classes is a challenging aspect for many prediction tasks and the adoption of language descriptions could provide further breakthroughs. The results are presented in Table 9 and Table 10. We report the classification-only results (without conditioning on a correct box prediction) because we want to highlight the substantial classification improvements owed to improved semantic understanding. The corresponding metrics are denoted as NO and VO respectively.

Model	NO \uparrow	Top-10 NO \uparrow	Tail NO \uparrow
Ego4D	28.70	27.58	26.45
TransFusion	33.80	31.84	32.37
Improvement	18%	15%	22%

Table 9. **Noun-only mAP** for top 10 and tail noun categories on Ego4D dataset. We observe consistent gains over the full class spectrum, in particular in tail classes.

Model	VO \uparrow	Top-5 VO \uparrow	Tail VO \uparrow
Ego4D	5.22	10.11	4.38
TransFusion	12.00	23.54	11.46
Improvement	129%	132%	161%

Table 10. **Verb-only mAP** for top 5 and tail verb categories on Ego4D dataset. We observe consistently strong gains over the full class spectrum, in particular in tail classes.

Model performance dependence on bounding box size. We additionally present a performance comparison based on the size of the ground-truth bounding box. We divide the ground-truth labels into 3 categories according to their area, each one containing a third of the total validation samples. The results for the Box-Noun mAP metric are shown in Table 11. We again notice consistent improvements across the different categories, which show that our method is flexible enough to perform well on difficult cases such as small bounding boxes or tail classes. This is encouraging because improving on these corner cases usually requires a lot of effort. The TransFusion model using language action context summaries achieves this without any special design choices aimed towards improving this objective.

With respect to the Box-Noun-Verb mAP, we notice regular gains of about 1.5 points over the Ego4D methods (hence, this result is omitted from the table). This suggests that the verb label prediction is more dependent on understanding the scene and action context in a holistic manner.

Model	Ns \uparrow	Nm \uparrow	Nl \uparrow
Ego4D	6.39	15.20	21.82
TransFusion	7.91	18.65	22.75
Improvement	23%	22%	4%

Table 11. **Box-Noun mAP** for small (Ns), medium (Nm) and large (Nl) boxes. Box-Noun-Verb mAP improvement is about 1.5 points for each of the categories hence it is omitted. Our method improves detection and classification results on difficult cases with small bounding boxes, complementing the hard to encode visual cues.

11. Architecture ablation

11.1. Visual encoder

The visual encoder ablations presented in the main paper section are realized using a simpler setup where the augmentation scale higher range for MobileNetV3 is limited to 480x640 (sizes given in height-first notation). For the ResNet-50 runs, we do not use any scale augmentation, fixing the input resolution to 768x1024.

11.2. Language encoder

Language Encoder	Token size	N \uparrow	N-V \uparrow
SBERT/BERT	384	20.09	7.62
SBERT/RoBERTa	768	19.78	7.78
SBERT/RoBERTa*	768	18.16	7.21
GPT-2	768	18.98	7.08
Flan-T5	1024	18.26	6.61

Table 12. **Language encoder ablations.** We compare SBERT using BERT and RoBERTa backbones with different language encoders, GPT-2 and Flan-T5. In the table, we include the original token size output by each language encoder. In this experiment, we project the output tokens to an embedding of dimension 768 before fusion. We report Top-5 Noun (N) and Noun-Verb (N-V). * Denotes the run without any language encoder finetuning. TransFusion is competitive even without finetuning the language encoder, recording only a small performance drop.

We reproduce Table 4 in Table 12, where we include an experiment with the SBERT/RoBERTa language encoder without any finetuning. This run achieves a Box-Noun mAP of 18.16 and a Box-Noun-Verb mAP of 7.21. The results are about 1 and 0.5 points lower than the finetuned variant, with no relevant decay in Box AP. While the gap is not extreme, it shows that a certain degree of input domain adaption is required for the language encoders. We consider this to be caused by the difference in syntax between the generated summaries and what is found in native texts. In spite of the use of natural language descriptions, our context construction is quite structured and could be more difficult to represent for models without being finetuned. Some relevant context summaries are illustrated in section 14. For this ex-

perimental setup, we use a context length of 2 for \mathcal{A} and include 3 visible object labels \mathcal{N}_v in the context summary.

11.3. Learning scale-specific features

Shared multiscale fusion weights. An alternative take to combat overfitting is to share model weights over multiple similar inputs, such that they are forced to learn more general data representations. We apply this principle by resharing the transformer fusion weights over the multiple input scales. Because this setting imposes additional constraints on the fusion weights, we increase the fusion module’s capacity by 33% (such that it still fits on one of our GPUs) and reduce the L2 weight decay to $3e-5$ to allow more optimization freedom. Using this setup, we register a notable decrease in performance. We perform multiple runs, but do not manage to score more than 7 MAP Box-Noun-Verb and 18.7 MAP Box-Noun on the validation set (approximately .5 and 1.5 absolute point difference). This indicates that using shared fusion weights at multiple scales is counter-productive for our task and that the model learns different representations at different feature map scales, all needed for effective prediction. The other hyperparameters are kept fixed as in [section 8](#), with a context length of 3 used for \mathcal{A} .

Forwarding language features. Instead of copying the language encoder outputs for every scale-level fusion, we forward the corresponding fused tokens to the latter stages. Additionally, we also append residual connections between the language features tokens at the successive multiscale levels to allow the model to more easily retain some of the initial information. The results are presented in [Table 13](#) where we notice the improved results obtained with the “copy” strategy as opposed to reusing features from previous scale levels. This further supports our hypothesis that each scale level operates with distinct, specialized representations and that reusing ones from different scales is detrimental to model performance. For this experiment, we use the parameters described in [section 8](#) with a context length of 3, including visible objects.

Forwarding strategy	N \uparrow	N-V \uparrow
Copy	19.69	7.50
Simple forward	18.97	7.27
Residual forward	18.38	6.96

Table 13. **Language feature forwarding strategy comparison.** We report Top-5 Noun (N), and Noun-Verb (N-V) for different language feature forwarding strategies using a context length of 3. Copying the language features at each fusion level lets the model derive specialized features that help performance.

11.4. Language modeling loss

We also investigate including an additional language model loss to further accelerate the action label learning. Specifically, we include an additional loss term, $\mathcal{L}_{lm} = \frac{1}{2}(\mathcal{L}_{lm_N} + \mathcal{L}_{lm_V})$ in the final optimization objective

$$\mathcal{L} = \mathcal{L}_{box} + \mathcal{L}_{noun} + \mathcal{L}_{verb} + \mathcal{L}_{ttc} + \mathcal{L}_{lm} \quad (15)$$

The target categories for this loss are the ground-truth noun and verb labels; \mathcal{L}_{lm_N} and \mathcal{L}_{lm_V} are regular cross-entropy losses. The difference between \mathcal{L}_{noun} , \mathcal{L}_{verb} and \mathcal{L}_{lm} is that the later term is applied on the mean-pooled *fused language tokens* at each multiscale fusion level (i.e. the transformer encoder outputs). The former ones work on the ROI-pooled bounding-box features in the Faster R-CNN prediction heads. The experimental results however did not show any improvement when including \mathcal{L}_{lm} , which instead decreased the final Box-Noun-Verb performance. We believe that this task in itself can be quite challenging. Without considerably increasing the model capacity, performing it concomitantly with the detection-based objectives can negatively impact the target model’s performance.

12. Video features and context length

To perform the context length comparison, we use the default parameters presented in [section 8](#). To further confirm our findings, we perform an additional run with a video context length of 6, which covers more than 100 frames before the prediction moment. We find that this does not bring any additional performance boost compared to the runs presented in [Figure 5](#) from the main section. It registers a top-5 Box-Noun mAP performance of 18.83 (more than 1 point below the average summary-based run) and 6.40 Box-Noun-Verb mAP (also about 1 point lower). This generally agrees with results presented by the Ego4D paper in their [Table 39](#), where the improvements from increasing the number of SlowFast clips suffer slightly diminishing returns. While this work is not an exhaustive comparison of different types of video feature extractors, SlowFast features are still considered effective enough to be used for the latest works, including the Ego4D 2nd-stage, hence we consider them a relevant baseline. Finally, when contrasted with the language encoder run without finetuning presented in [Table 4](#), the difference in Box-Noun-Verb mAP is 0.8 points (or about 12%). We consider this to be relevant enough to show the benefit of using language descriptions even when not finetuning the language encoder.

13. EPIC-KITCHENS 100

Dataset preparation The SlowFast features for the EK100 dataset are extracted with an 8x8 ResNet-101 SlowFast backbone pre-trained on the Kinetics 400 dataset [[25](#)],

using a stride of 16 frames and a window size of 32 frames. This replicates the extraction procedure for the Ego4D-provided features to ensure comparability. We emphasize that the EK100 dataset only provides low-resolution images of 256x456 (that we upsample to 480x640; sizes given in height-first notation) which makes the prediction task even more difficult. This is confirmed by the presented metric values, more in line with the low-resolution Ego4d MobileNetV3 runs. A certain degree of noise in the ground-truth bounding boxes generation can be expected. In some cases, there are multiple matching object detections; hence we use the model confidence score to break ties and choose the bounding box with the largest value.

On average, the EK100 scenes are much more cluttered and more difficult to interpret than the Ego4D ones because of the several objects that could be interacted with in a kitchen. Kitchen scenes represent only 11% of the Ego4D dataset and we do not expect our model to excel in those environments more than the others, hence we consider EK100 to be a different benchmark.

13.1. Additional results

We extend Table 5 from the main section with additional metrics to provide more insight into how the models perform on EK100 in Table 14. Namely, we exclude the noisy bounding box prediction when computing the Noun-Only (NO) and Verb-Only (VO) top-5 mAPs such that we can evaluate the noise-free label prediction.

Finetuning results We further include results achieved by finetuning an Ego4D-trained TransFusion model. We freeze all the layers with the exception of the prediction heads. Using this strategy, we manage to obtain competitive results, on par with the training-from-scratch performance when trained for a limited amount of epochs. For prolonged training sessions, the from-scratch versions eventually overtake the finetuned ones. The verb prediction task translates better to the EK100 domain since the verb categories used by the two datasets are somewhat comparable. On the other hand, noun prediction requires different features because of the large domain gap between the two datasets, which explains the reduced finetuning performance of noun prediction. The results support our claim that using language to describe past action context is an effective alternative for interaction forecasting tasks, even for difficult datasets.

Language encoder choice According to our experiments, the choice of language encoder is more significant for EK100, where the larger SBERT/RoBERTa language encoder seems to be better suited. We hold that this is due to the fine class differences that must be understood by the model: salad vs. parsley, drink vs. bottle, bean vs. nut, and lemon vs. fruit. This requires a more expressive

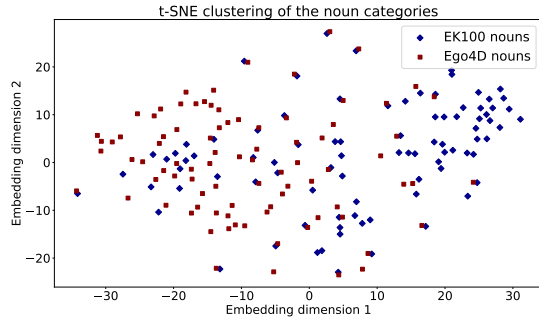


Figure 7. **t-SNE embedding of the noun categories for the two datasets.** A sizeable cluster of the EK100 nouns can be noticed on the right, while the Ego4D noun categories are more grouped towards the left. This shows the domain gap between the two datasets for noun categories.

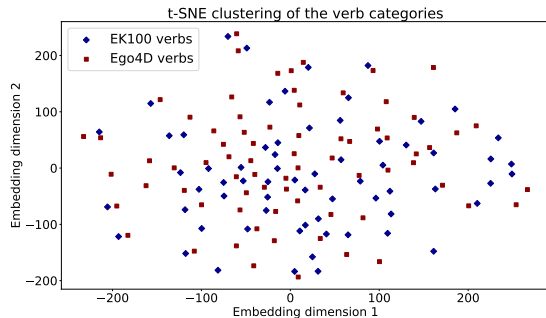


Figure 8. **t-SNE embedding of the verb categories for the two datasets.** The verbs are more uniformly spread and cover approximately the same space, which makes transfer learning easier.

and powerful language encoder to pick up the finer details, whereas a coarse understanding was enough for Ego4D, since its classes are more semantically distinct. We obtain a 0.5 Noun-Verb increase when switching from the small SBERT/BERT to SBERT/RoBERTa version and a 1.0 Noun increase. These numbers are notably larger than the 0.16/0.4 reported for Ego4D in Table 4.

To support our claims, we visualize the clustering of the noun and verb categories after applying the t-SNE dimensionality reduction method [44] on the corresponding 300-dimensional GloVe [34] embeddings. In Figure 7, we notice a sizeable cluster of the EK100 nouns on the right-hand side, while the Ego4D nouns tend to be clustered on the left-hand side. Hence, transfer learning for noun classification is less likely to perform adequately. We also notice the small distance in the embedding space for the noun classes (especially the EK100), which reinforces the difficulty of separating them. Verb clustering is presented in Figure 8, where we can observe a much larger overlap between the

two datasets’ classes and easier separability given the larger distances between them.

14. Qualitative results

We present in Figure 9 and Figure 10 a qualitative comparison between our method and that of Ego4D, using a context length of 3 for action verb-noun pairs \mathcal{A} and 3 visible objects \mathcal{N}_v for our language-aided model. The green bounding box represents the ground truth location of the next object interaction. The white text represents the input action summary context description: the first row represents the visible objects and the second the captioned action labels. We show the top-4 most confident bounding box predictions and their associated noun, verb, and TTC estimates.

Model	N \uparrow	N-V \uparrow	NO \uparrow	VO \uparrow
TransFusion GT	6.47	2.58	23.27	7.78
TransFusion Summary	4.26	1.63	9.83	5.39
TransFusion Summary \dagger	3.28	1.16	6.61	5.12
TransFusion Summary *	3.83	1.60	11.64	8.43
TransFusion-Video	4.02	1.66	8.75	6.13

Table 14. **Object interaction anticipation on EK100.** EK100 results using generated ground-truth (GT), generated summary, and video features. We report Top-5 Noun (N) and Noun-Verb (N-V) used by the Ego4D challenge, the Noun-Only Top-5 mAP (NO) and Verb-Only Top-5 mAO (VO) where we *do not* condition on a correct bounding box prediction. The EK100 dataset is more difficult to process, especially because of the fine grained noun categories. Hence, TransFusion requires a stronger language encoder to be competitive. The transfer-learning gains are larger for verbs, since they overlap more with the Ego4D dataset. * Denotes the model with *finetuned* classification and box regression heads, and frozen backbones, fusion, region proposal/pooling layers. \dagger denotes the model trained with the small SBERT/BERT variant, all the others (except TransFusion-Video) are trained using SBERT/RobBERTa.

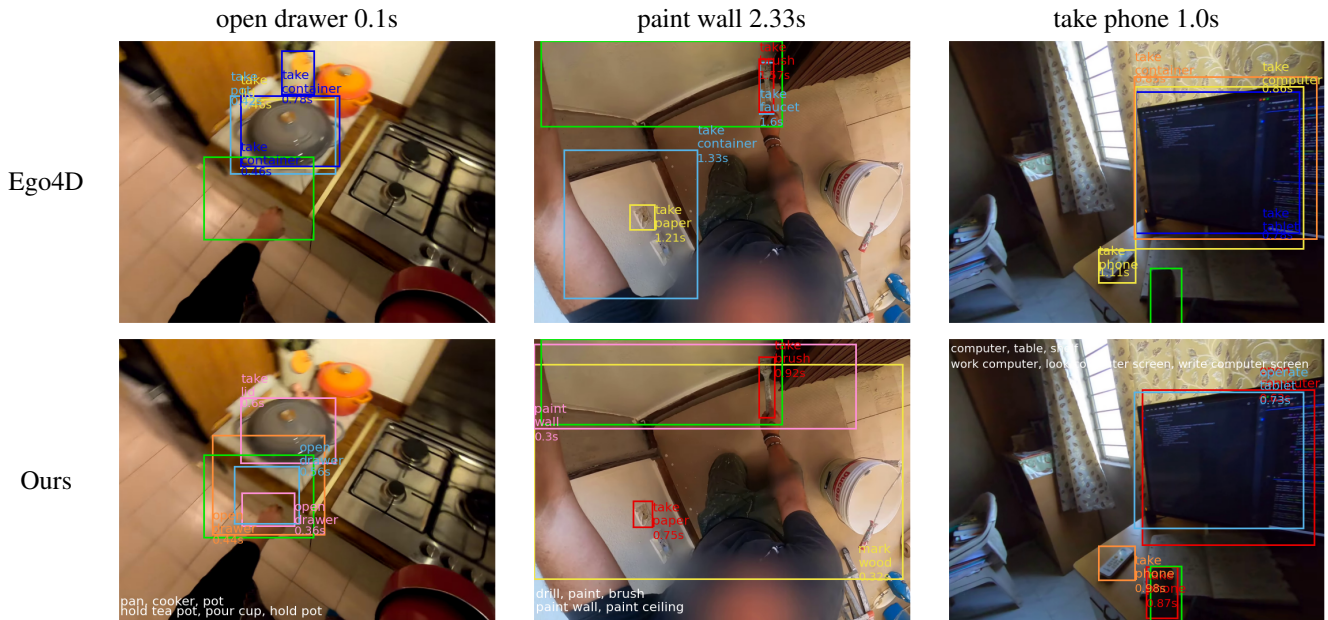


Figure 9. **Qualitative examples of Ego4D and TransFusion (ours) predictions.** The ground-truth action label and TTC is represented on top of each column. The bright green bounding boxes denote the ground-truth location of the next object interaction. Action contexts used as language input in TransFusion are shown at the bottom in white. On average, our model manages to get more accurate predictions.

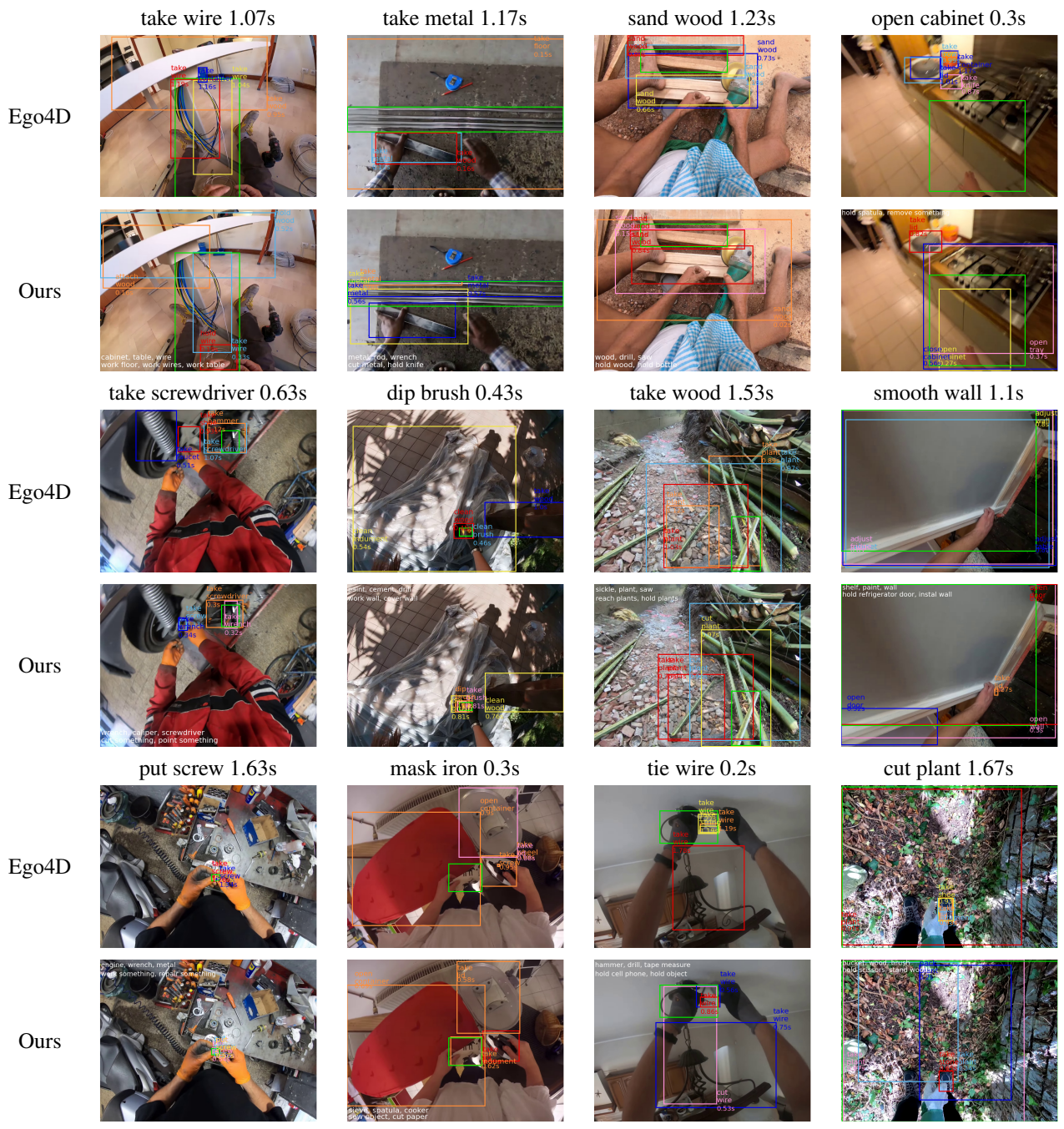
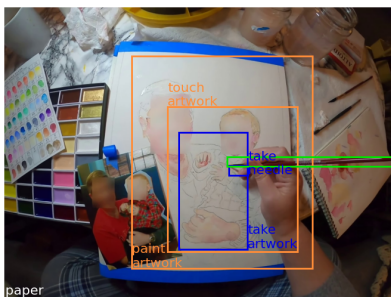
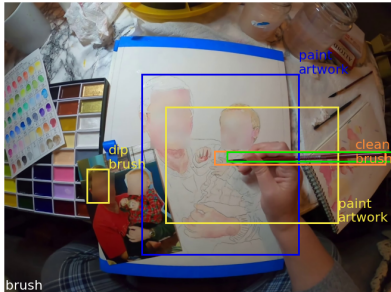
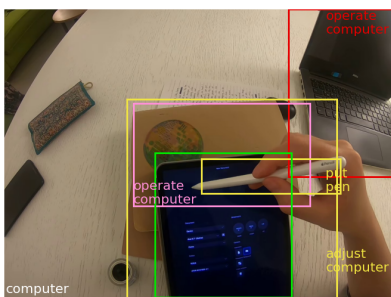
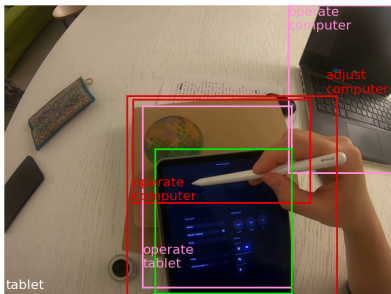


Figure 10. **Additional qualitative examples of Ego4D and TransFusion (ours) predictions.** The ground-truth action label and TTC are represented on top of each column. The bright green bounding boxes denote the ground-truth location of the next object interaction. Context summaries used in TransFusion are shown at the bottom in white. On average, our model manages to get more accurate predictions.

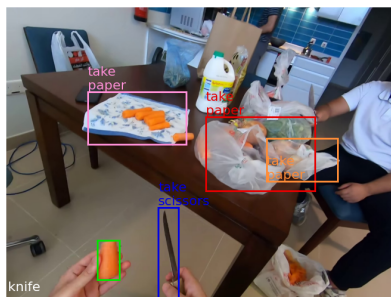
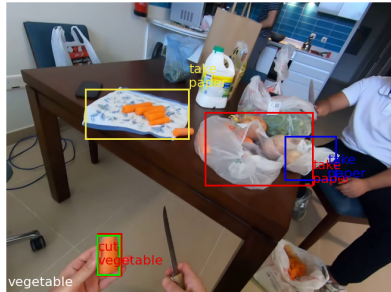
Changing the model predictions by changing the language input from *brush* (top) to *paper* (bottom)



Changing the model predictions by changing the language input from *tablet* (top) to *computer* (bottom)



Changing the model predictions by changing the language input from *vegetable* (top) to *knife* (bottom)



Changing the model predictions by changing the language input from *bicycle* (top) to *wrench* (bottom)



Changing the model predictions by changing the language input from *car* (top) to *paint* (bottom)



Changing the model predictions by changing the language input from *dough* (top) to *food* (bottom)

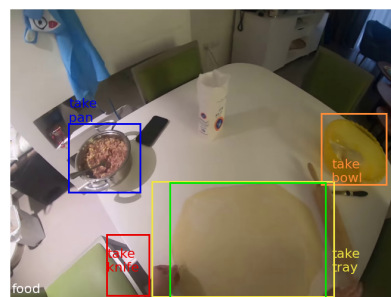
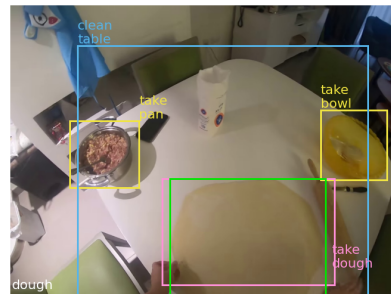


Figure 11. **Additional qualitative examples of predictions when changing the language input.** Our model modifies the predicted labels and locations *dynamically* based on the input language context descriptions. We show the input language context in white, in the bottom left corner of each image.